

WHAT LOCAL MAGNETIC FIELDS CAN TEACH US ABOUT A POSSIBLE SUPERNOVA REMNANT (G182.5-4.0)

P. SINGH,¹ J. L. WEST,¹ AND J. L. CAMPBELL¹

¹*Dunlap Institute for Astronomy & Astrophysics, University Of Toronto, 50 St George St, Toronto, ON M5S 3H4*

ABSTRACT

This project focuses on classifying a currently unknown object which we refer to as G182.5-4.0. From current studies, it is believed that this object falls into one of two categories; an old supernova remnant in an unusual environment, or filaments in the interstellar medium produced by one or more supernova remnants which have retained their shape due to an interstellar magnetic field. We say that the object is a possible supernova remnant because of its highly unusual shape which does not comply with any current and commonly known geometries of supernova remnants. We believe that the unusual shape is connected and can be explained from the properties of the interstellar magnetic field which is suspected to permeate the object, and also the surrounding neutral hydrogen fibers. In this project, two algorithms known as the Rolling Hough Transform (RHT) and Rotation Measure (RM) Synthesis are used. The RHT and RM-Synthesis are able to provide connections between the orientation of the object and the magnetic field in distinct mediums. This way, it is possible to study any connections between these orientations through two different methods. To display these results, orientation maps in the form of polar plots and a line integral convolution map have been generated. From these orientation maps, a strong connection between the shape of G182.5-4.0 and the direction interstellar magnetic field at the orientation angle of $101^\circ \pm 12^\circ$ with respect to the polar plot coordinate axes has been made. Therefore, there is strong evidence that this interstellar magnetic field has played a vital role in determining the structure of G182.5-4.0.

1. INTRODUCTION

Magnetic fields are presumed to be pervasive in all parts of the Universe and are spread through almost all celestial objects and the medium in between (Han, 2017). For the case of large scale objects (and so to the scale of objects considered in astronomical observations), magnetic field strengths are generally on the order of a few μG (Ferriere, 2012) and are often in very complex orientations. This implies that these magnetic fields are difficult to quantify when attempting to conduct observations directly. The outstanding questions are then what other techniques can we use in order to better understand these magnetic fields? What can they tell us about the objects which are permeated by them?

1.1. *Background*

In this research project, the aim is to answer these questions for a possible new supernova remnant (SNR) located near the Crab Nebula, but presumed to be unassociated due its distance and size, called G182.5-4.0 (West et al., 2020). In Fig. 1, we display G182.5-4.0 through the total intensity parameter, which in this case, displays this object's shape very well (as com-

pared to the other parameters which will be discussed in Sec 2.1). G182.5-4.0 displays characteristics of being a shell that is very compressed, thin, and straight. These qualities disagree with the characteristics that conventional SNRs demonstrate (Igumenshchev et al., 1992). Typically, SNRs in the interstellar medium (ISM) frequently display characteristics of either disk symmetry (shell elongated in a disk structure) or spheroid attributions (shell extending in all directions exhibiting a somewhat closed spherical shape) (Igumenshchev et al., 1992). However, SNR geometry is not just limited to the previous two cases. It is possible for SNRs to exhibit all kinds of shapes and sizes. One thing that is usually common between most SNRs is the fact that their shape typically forms some kind of a closed structure (Lopez, 2013). In Fig. 1, G182.5-4.0 can be seen as having open ends which directly distinguishes its unique filament structure. The two prevailing hypotheses for what this object can possibly be are as follows:

1. An Old SNR: The object is in a bizarre configuration consisting of thin and elongated filaments. If this object indeed is a SNR, then it would suggest that its shell is very compressed and is due to its

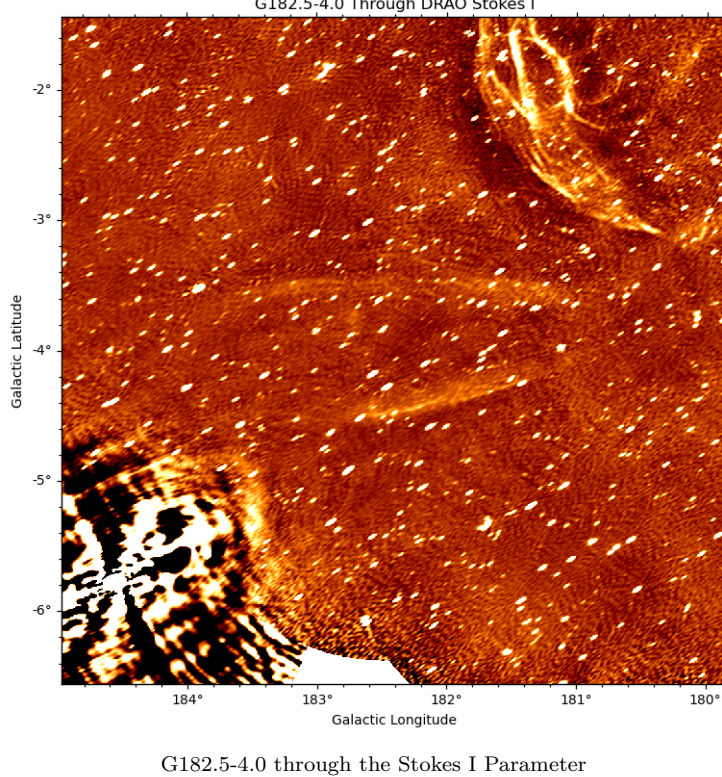


Figure 1. SNR candidate G182.5-4.0 near the Crab Nebula. This finding is a radio observation conducted by the Dominion Radio Astrophysical Observatory Synthesis Telescope (DRAO-ST). This image is a Stokes I total intensity measurement at 1420 MHz with a resolution of 1'. In this image, we can see some identifiable structures. One being the Crab Nebula which is located near the bottom-left and the other being S147 which is a faint shell type SNR (Xiao et al., 2008) located near the top-right. The object of interest lies in the center of the image perceived as unusual structure with a very compressed, thin, and straight shell. The bright intensity point sources in this image are due to external background galaxy intensity emissions and are ignored for the examination of this object.

presence in an unusual environment (West et al., 2020).

2. Filaments in the ISM: This object could also be a product of a very old or multiple SNRs which have achieved their elongated shape due to a Galactic magnetic field (West et al., 2020).

1.2. The Relativistic & Polarized Medium

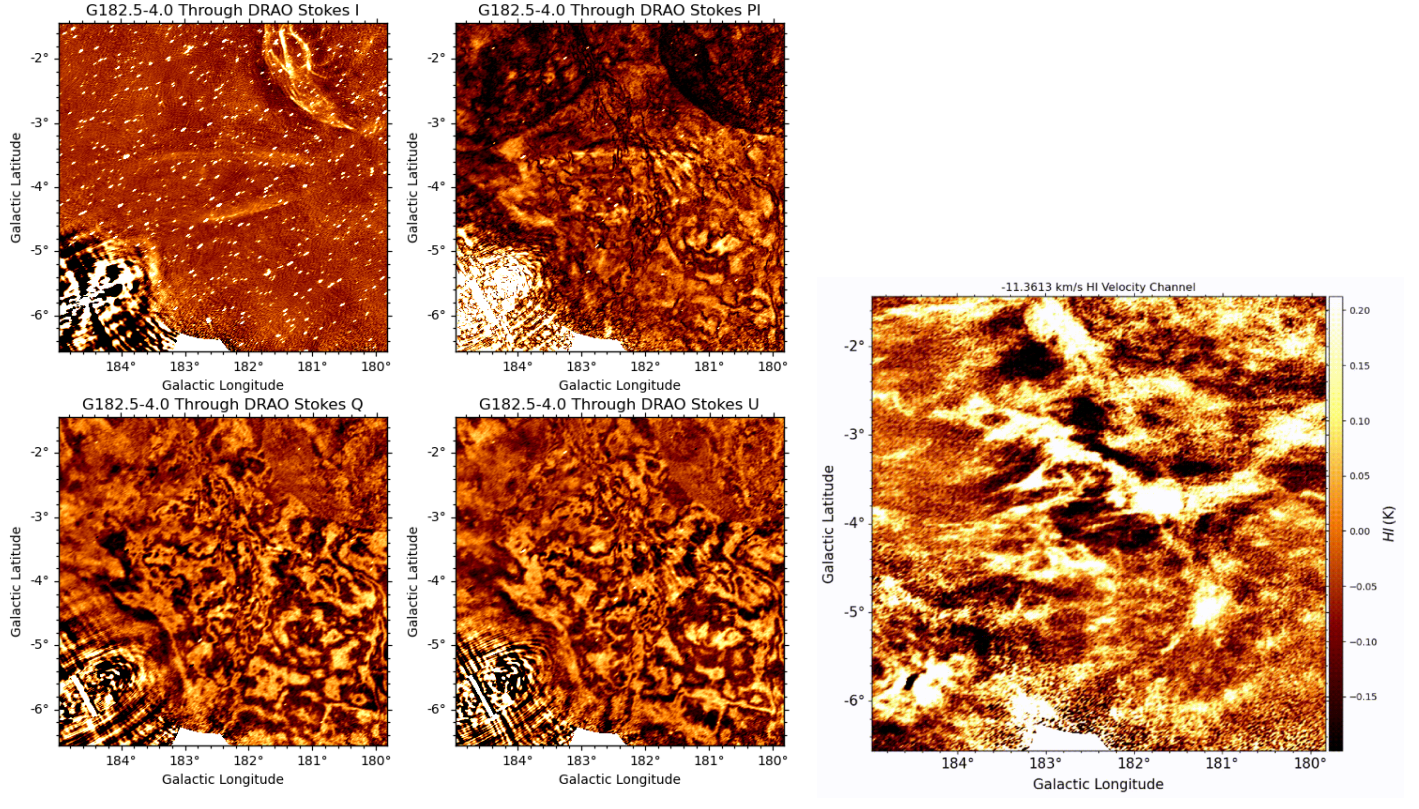
One way to provide conclusive evidence for the presence of a Galactic magnetic field is to study radio synchrotron radiation. Synchrotron radiation is the electromagnetic radiation emitted when charged particles are accelerated in a direction which is perpendicular to their velocity (Newton-McGee, 2009). Synchrotron radiation observed in galaxies originates from relativistic electrons which spiral perpendicularly to magnetic field orientations (Han, 2017). Therefore, if synchrotron radiation is observed, we know that there is a magnetic field present. Another connection between SNRs and synchrotron radiation is that the dominant radiation

emitted for SNRs is in fact synchrotron radiation which is intrinsically polarized (Han, 2017). From this, the object of study will be the most visible through radio observations. The observations used in this study are derived from the Dominion Radio Astrophysical Observatory Synthesis Telescope (DRAO-ST) and G-ALFA Continuum Transit Survey – Arecibo Telescope (GALFACTS) radio observations for G182.5-4.0 which will be discussed in more detail (Sec. 2).

1.3. The Neutral Medium

In the best case scenario, we would like to understand everything about the magnetic field which we know is encompassing this object. This includes its magnitude (strength) and orientation (direction). One of the ways in which one can begin to understand the orientation of the magnetic field is to study in particular the neutral hydrogen (HI) fiber regions coexisting with the object.

We know that there is a confirmed presence of a wind-blown HI bubble in the vicinity of this object (Wallace et al., 1999). When HI fibers are present in a magnetic



(a) G182.5-4.0 through the Stokes I, PI, Q and U Parameters

(b) A Particular HI Velocity Channel Near G182.5-4.0

Figure 2. DRAO-ST Stokes Parameter radio observations (a) and a single velocity channel of the HI cube data (b). In general, the HI cube of data contains multiple 2-dimensional data sets (images) separated by specific velocity channels. Image (a) contains the Stokes I Total Intensity (top-left), Stokes PI Total Polarized Intensity (top-right), and Stokes Q and U which are the Polarized Components of Stokes PI (bottom-left and bottom-right). All of the images in (a) and (b) were captured at a frequency of 1420MHz and a resolution of 1'.

field, they are known to align themselves along the direction of the interstellar magnetic field (Clark et al., 2014). This means that it is then possible to apprehend the orientation of the magnetic field. If this is the case and we have an indication of the orientation of the magnetic field, this can be compared to the orientation of G182.5-4.0 which in turn will provide evidence for the explanation of the structure of this object.

2. DATA

2.1. DRAO Data

The DRAO-ST is a 7-antenna radio telescope located in Kaleden, British Columbia. Operating simultaneously at the frequency of the spin-flip spectral line of atomic hydrogen (the HI line near 1420 MHz), and in two continuum bands near 1420 MHz and 408 MHz, the telescope achieves arcminute angular resolution with exceptional sensitivity to extended structure over wide fields (Landecker et al. 2000). This allows for the mapping of several major constituents of the ISM, namely

the atomic gas (through the HI line), the ionized gas (thermal continuum emission detected in the continuum bands), and the relativistic component (which generates synchrotron emission, measured in the continuum bands) in a way which few other telescopes can match (Landecker et al. 2000).

In this project, a single data set containing five image products was derived at a resolution and frequency of 1' and 1420 MHz respectfully. The five image products correspond to a Stokes total intensity (I) image (as in Fig. 1), the Stokes complex components of linear polarization (Q and U), and compiled series of HI images (Newton-McGee, 2009). The Stokes total polarized intensity (PI) is given through Stokes Q and U by $PI = \sqrt{Q^2 + U^2}$. The Stokes parameters as well as a single velocity channel of the HI data are shown in Fig. 2. In Fig. 2(a), G182.5-4.0 is shown through the various stokes parameters while in Fig 2(b) a single HI velocity channel of -11.3613 km/s is shown near G182.5-4.0. In general, the HI data is comprised of a

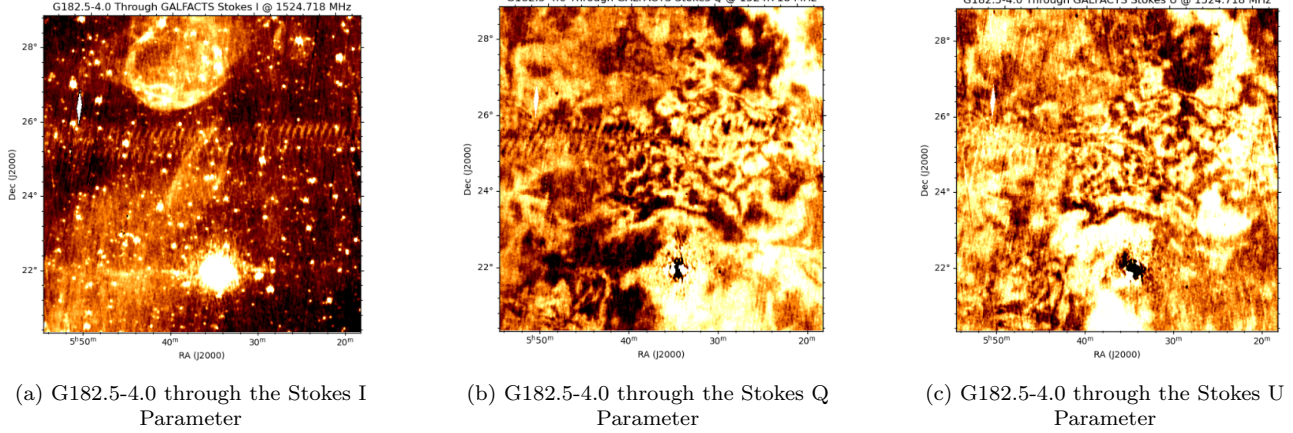


Figure 3. SNR candidate G182.5-4.0 near the Crab Nebula. This finding is a radio observation conducted by the G-ALFA Continuum Transit Survey – Arecibo Telescope (GALFACTS). This set of images contains a particular frequency channel of Stokes I total intensity, and Stokes Q and U Polarized Intensity component measurements. Although only one frequency channel is shown here, in general the frequency range of this data goes from 1370–1520 MHz with a resolution of $4'$. The object of interest lies in the center of the image perceived as unusual structure with a very compressed, thin, and straight shell. These images contain artificial data which can be seen as bright periodic linear structures which run across the images and can be ignored for the examination of this object.

data cube of multiple 2D images with velocity channels ranging from 28.2115 km/s to -43.5141 km/s with increments of -0.8244 km/s between each adjacent channel. Here, negative velocity refers to pointing away from the observer and positive velocity refers to pointing towards the observing as viewing along the line-of-sight.

2.2. GALFACTS Data

The GALFACTS - Arecibo Telescope is a 305m single dish telescope located in Puerto Rico. GALFACTS observations create full Stokes image cubes at an angular resolution of $4'$, with several thousand spectral channels covering 1225–1525 MHz, allowing sensitive imaging of polarized radiation and Faraday Rotation Measure from both diffuse emission and against a high density grid of extra-galactic sources (Taylor et al., 2010).

In this project, multiple data sets containing three image products were derived at a resolution of $4'$ and a frequency range of 1370–1520 MHz around G182.5-4.0. These three image products correspond to Stokes I, Q, and U. The key difference in the GALFACTS study is that it contains a range of frequency channels for each of the labelled Stokes Parameters while the DRAO-ST data contains a single frequency channel. In Fig. 3, we can look at a sample of the GALFACTS data for this project. Here, we can observe G182.5-4.0 through the labelled Stokes Parameters for a single frequency channel at approximately the upper limit of 1520 MHz. In general, each of the Stokes parameters in Fig. 3 are given through a frequency range of 1370 MHz to 1520 MHz with increments of 0.42 MHz between each adjacent fre-

quency channel. The difference in resolution between the GALFACTS and DRAO-ST data can be best seen through the Stokes I image of Fig. 1 where the resolution is greater than that of the Stokes I image of Fig. 3(a).

As mentioned in Sec. 1.2, the synchrotron radiation considered in both of the DRAO-ST and GALFACTS data sets is intrinsically polarized. The angle of this observed polarization of the synchrotron emission is given through the Stokes parameters as $\chi = \frac{1}{2} \arctan \frac{U}{Q}$ rad.

2.3. Other Data

We also consider the H-Alpha ($H\alpha$) Full Sky Map (Finkbeiner 2003) at a frequency of 456.79 THz in order to probe thermal electron densities, which will be discussed in more detail (Sec. 5). This data was collected by the Virginia Tech Spectral Line Survey (VTSS) in the northern hemisphere and Southern $H\alpha$ Sky Survey Atlas (SHASSA) in the southern hemisphere. The raw $H\alpha$ map around G182.5-4.0 can be seen in Fig. 4. In Fig. 4, a darker colour represents stronger intensities of $H\alpha$ corresponding to that particular region.

3. METHOD

3.1. The RHT

HI fibers are known to have a deep connection with magnetic fields. In particular, it is known that in the presence of a magnetic field, regions where HI is present will undergo a shift in orientation such that they are then aligned with the magnetic field (Clark et al., 2014). This is an extremely useful property that can aid in

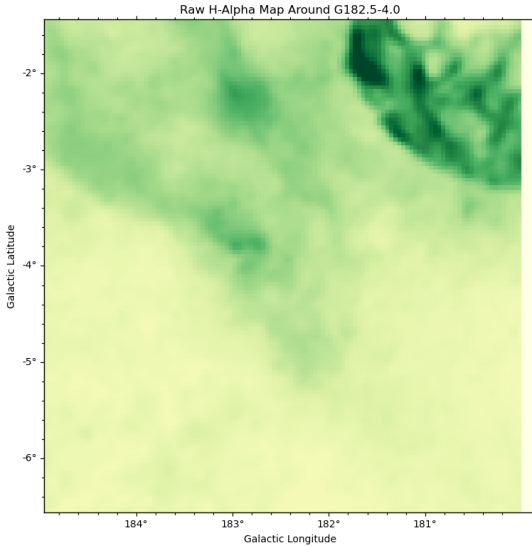


Figure 4. Intensity of H α near G182.5-4.0. This image is a part of the H α Full Sky Map captured at a frequency of 456.79 THz. Higher intensities of H α are denoted by a darker green hue.

determining the presence of magnetic fields that would otherwise be difficult to observe and study directly.

We would like to have a more quantitative way to monitor and provide a deeper analysis for these HI structures. For this, we introduce the Rolling Hough Transform (RHT). The RHT is an algorithm that quantifies the linearity and spatial coherence of HI structures (Clark et al., 2014). It does so through running a specific algorithm through the coding software Python which is able to detect these fibers in a data set and then presents a new data set which traces their orientation (Clark et al., 2014).

Since HI fibers have the unique property of aligning with the magnetic field (Clark et al., 2014), it is possible to infer details about the orientation of such a magnetic field and begin to understand some of its spatial properties. Once there is an idea about the features of the magnetic field, we can then determine if G182.5-4.0 has any type of relation to the encompassing HI fibers and therefore to the magnetic field orientation.

3.2. RM-Synthesis

3.2.1. Faraday Rotation

Before explaining the method of Rotation Measure (RM) Synthesis, we first discuss a key phenomena known as Faraday Rotation. Recalling from Sec. 1.2, synchrotron radiation is emitted when high-speed electrons spiral around magnetic field components. Since the magnetic field components in which these electrons travel along contains a definitive direction, this means that the

synchrotron radiation which is emitted during this process is polarized in a direction which depends on the intrinsic magnetic field component from which it originated. When attempting to probe the magnetic field orientation from this connection between the polarized synchrotron emission and the intrinsic magnetic field, on occasion, that magnetic field orientation can be rotated (Brentjens et al., 2005). This effect is called Faraday Rotation. Faraday Rotation is an effect in which the orientation of a magnetic field is observed to be rotated from its intrinsic orientation, as probed by the synchrotron radiation which originates from it (Brentjens et al., 2005).

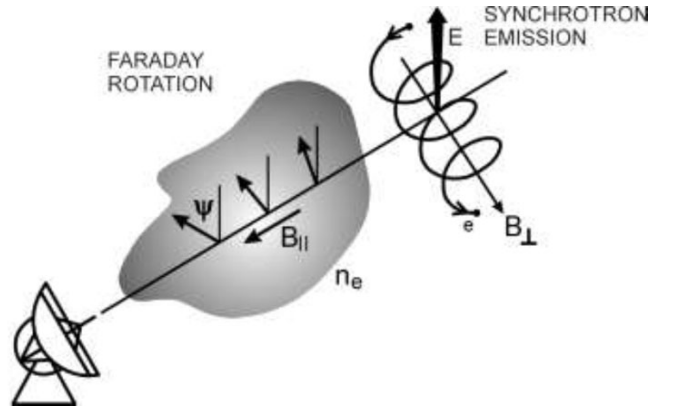


Figure 5. An image depicting the effect of Faraday Rotation. In this image, B_{\perp} shifts in orientation by ψ as it passes through a line-of-sight magnetic field (B_{\parallel}) and thermal electron region. An observer will measure B_{\perp} to be rotated an angle of ψ with respect to the intrinsic magnetic field direction from which the radio synchrotron emission originates.

Fig. 5 displays the process of Faraday Rotation. In this figure, we see the perpendicular component of the magnetic field (B_{\perp}) being rotated by an angle (ψ) as it passes through the parallel component (B_{\parallel}) of that magnetic field and a thermal electron density region (n_e). The rotation angle (ψ) can be probed by the angle of polarization of the synchrotron emission which an observer would see. The thermal electron density also plays a role in Faraday Rotation and will be discussed in the next section.

3.2.2. Rotation Measure

Through studying the process of Faraday Rotation, it is possible to determine the de-rotated plane-of-sky (POS) magnetic field orientation. This is done through an algorithm known as RM-Synthesis which determines a quantity called Rotation Measure represented as RM . Formally, RM is given by the following formula:

$$RM = 0.81 \int_{source}^{observer} n_e \vec{B} \cdot d\vec{l} \quad (1)$$

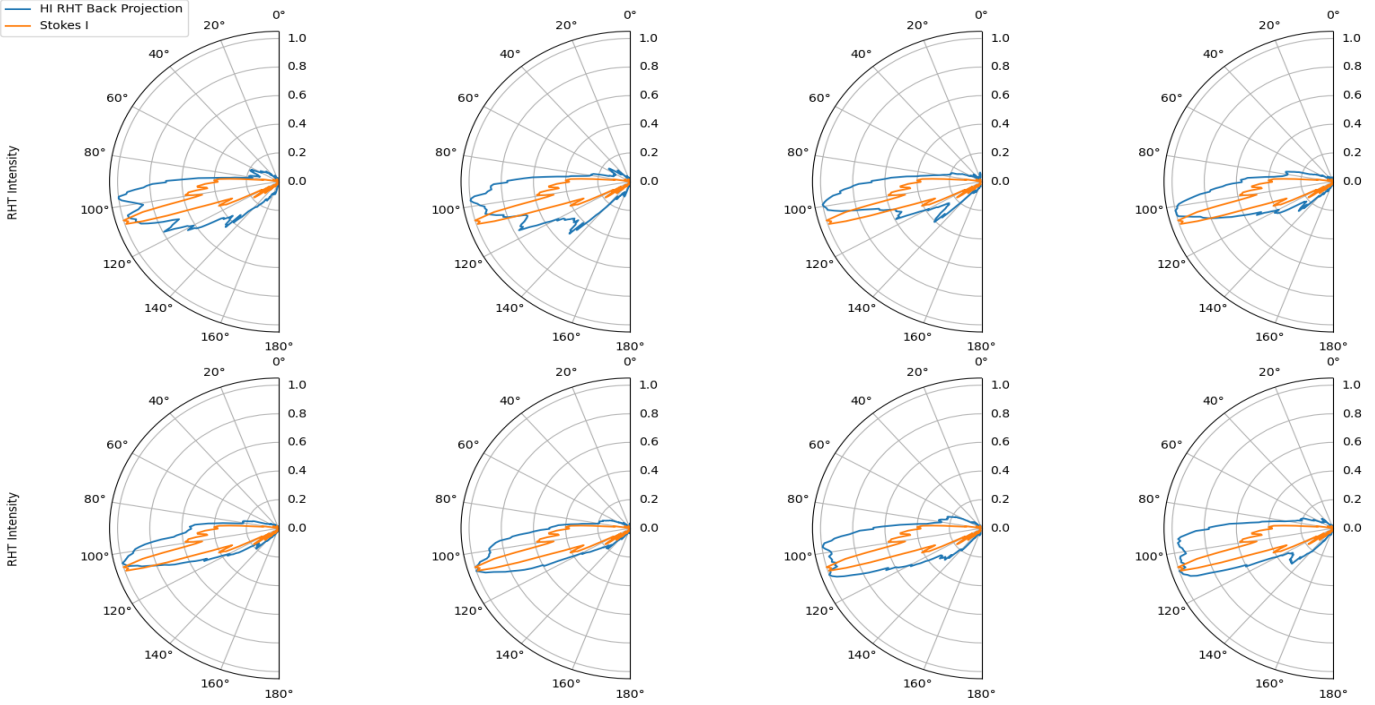


Figure 6. The integrated (average) RHT orientation angles from the HI velocity channels of -4.7658 km/s, -5.5902 km/s, -6.4147 km/s, -7.2319 km/s, -8.0635 km/s, -8.8880 km/s, -9.7124 km/s, and -10.5368 km/s respectively (blue). These velocity channels were chosen in particular to illustrate the strong connection to the orientation of G182.5-4.0 (orange).

were RM is the rotation measure ($\text{rad} \cdot \text{m}^{-2}$), n_e is the thermal electron density (m^{-3}), \vec{B} is the magnetic field (μG), and $d\vec{l}$ is the infinitesimal path length (pc). RM tells us how strong the effect of Faraday Rotation is for a certain region (Heald, 2008). This means higher values of $|RM|$ indicate a stronger effect of Faraday Rotation. The sign of RM depends on $\vec{B} \cdot d\vec{l}$, and since we define the path to be from the source to the observer, this means that negative values of RM are produced by the LOS \vec{B} which point towards the observer and positive values of RM are produced by the LOS \vec{B} which point away from the observer.

In this project, we use an algorithm known as RM-Synthesis in order to determine RM values and the intrinsic POS magnetic field for the region around G182.5-4. Knowing the RM for a certain region allows one to unravel the effect of Faraday Rotation in order to determine the true orientation of the POS magnetic field. Formally, this is done through the following procedure:

$$\chi(\lambda^2) = \chi_0 + RM\lambda^2 \quad (2)$$

where $\chi(\lambda^2)$ is the observed angle of orientation of the magnetic field (rad), χ_0 is the intrinsic angle of orientation of the magnetic field (rad), and λ is the wavelength (m) which is given through the frequency (frequency channels of the data being used). RM-Synthesis requires polarized radio emission data from a range of frequen-

cies as input parameters in order to calculate RM values (Brentjens et al., 2005). By feeding in the GALFACTS data as mentioned in Sec. 2.2, the RM values can be determined for the region of space surrounding G182.5-4.0.

Along with calculating RM values, RM-Synthesis also provides angle data of the de-rotated (χ_0) angle values using Eq. 2. Using this angle data, it will be possible to generate a map which contains the intrinsic POS magentic field orientation. The goal will then be to compare this POS magentic field orientation to the previous HI fiber alignments in order to draw connections between the magnetic field orientations within these distinct mediums. From these connections, we will be able to determine if the interstellar magnetic field is playing a role in the orientation of the filamentary structure which we observe G182.5-4.0 to possess.

4. RESULTS

4.1. RHT Results & Polar Plots

The RHT was run on each HI velocity channel as well as the DRAO-ST Stokes I image in order to view filamentary structures. An example of this can be seen in Fig. 7. In this figure, the RHT output data, called a back-projection, for a particular velocity channel can be seen. These back projections contain the filamentary structures from the original data set which was inputted

into the RHT. The RHT was also run on the DRAO-ST Stokes I image from Fig. 1. This is because we can then have a way to track the filamentary structure of G182.5-4.0 in order to compare these orientations to those of HI filaments.

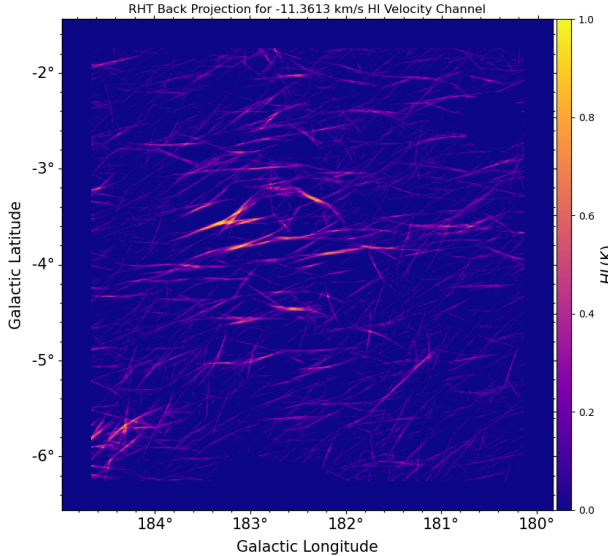


Figure 7. The RHT back-projection of the -11.3613 km/s HI velocity channel. This back-projection is the RHT output of the HI velocity channel from Fig. 2(b). We can see the ability of the RHT to determine filamentary structures from a given data set.

In order to quantify the orientations obtained from the RHT, we use polar plots which can be seen in Fig. 6. These polar plots were generated by determining the integrated (or average) orientation of the RHT back-projections for each of the HI velocity channels and then plotting the result. Alongside each of the integrated HI orientations, the integrated Stokes I orientation was also over-plotted. This was done so that the orientation of HI for a particular velocity channel could be compared to the orientation of G182.5-4.0. For this project, the reference angle of 0° is given from the upward vertical axis and increasing angles are then given in a counterclockwise orientation until the maximum angle of 180° is obtained (the same as the polar plots of Fig. 6). From Fig. 6, it can be seen that for the truncated range of velocity channels between -4.7698 km/s and -10.5368 km/s , we are able to observe a strong overlap (particularly in the -8.888 km/s velocity channel) between the orientation of G182.5-4.0 and the orientation of the HI fibers and hence the magnetic field.

From this, it has been determined that for particular HI velocity channels, the HI fibers for those velocity channels are aligned in a similar orientation to G182.5-

4.0. Since we know that HI fibers tend to align with interstellar magnetic fields (Clark et al., 2014), this result provides strong evidence that the filamentary structure of G182.5-4.0 is being influenced by the magnetic field which is permeating the region around G182.5-4.0. Taking the average integrated orientation of a range of well aligning HI velocity channels and performing basic statistical analyses produces an orientation angle of $101^\circ \pm 12^\circ$.

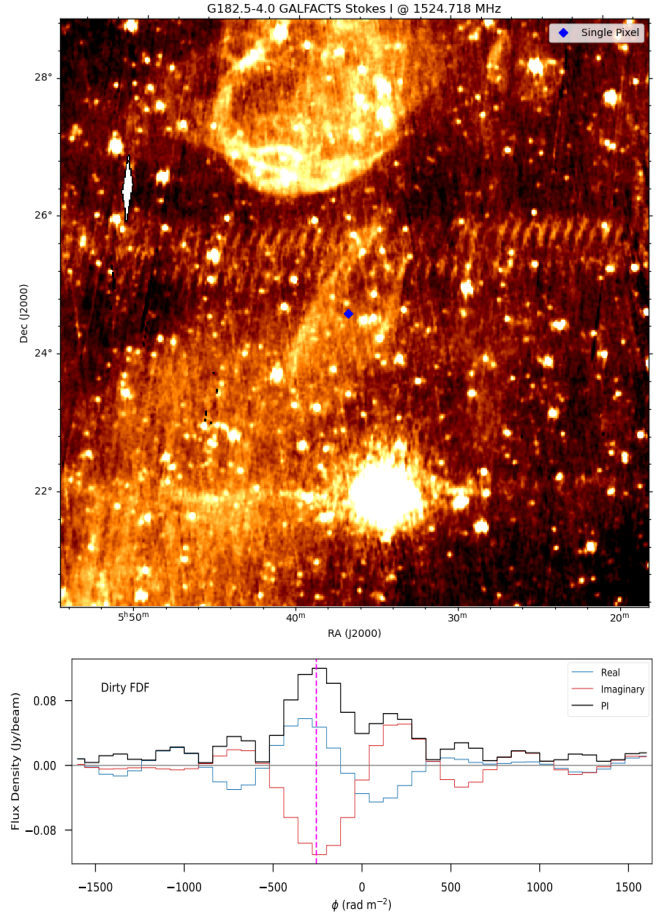


Figure 8. The 1D RM-Synthesis spectra plot (bottom) for a single pixel located at $(5h36m46s, 24^\circ 40')$ (top). The value of most interest is given by the dashed line indicating the peak of the RM , which in this case would be close to the value of -250 . This describes the effect of Faraday Rotation along the LOS for a single pixel.

4.2. 1D & 3D RM-Synthesis

For this project, RM-Synthesis was performed in two parts. The first part includes a 1D RM-Synthesis which is then generalized to a 3D RM-Synthesis. In this section, we provide the results of running both of the 1D and 3D RM-Synthesis for the given GALFACTS data.

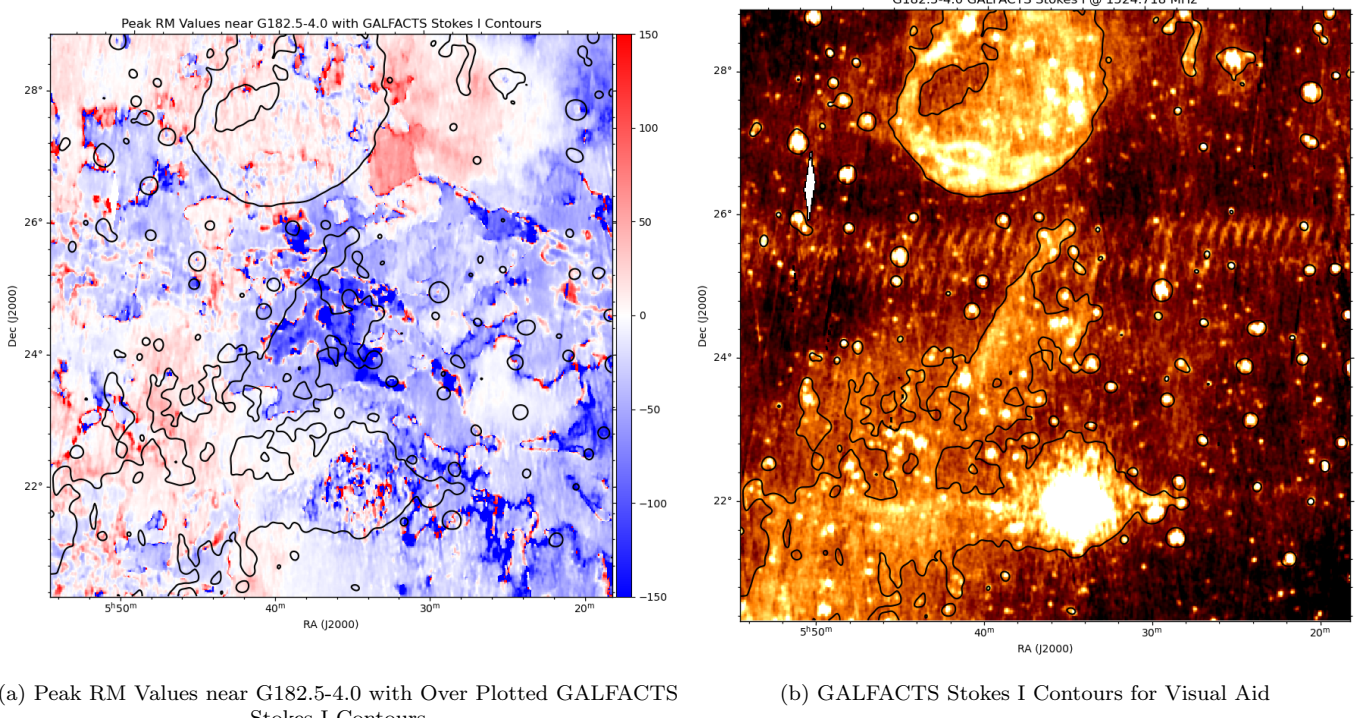


Figure 9. The 3D RM-Synthesis map with contours of G182.5-4.0 as seen through GALFACTS Stokes I for visual aid (a). The 3D RM-Synthesis map is a generalized procedure of the 1D RM-Synthesis procedure, in terms of determining the peak values of the RM for each pixel in a given data set. The peak RM values have been scaled around values of -150 - 150. This allows the map to display regions with none to little RM effects as white, while regions of red and regions of blue indicate high positive or high negative peak RM values respectfully. Also included is the GALFACTS Stokes I image (b) for visual aid.

4.2.1. 1D RM-Synthesis

1D RM-Synthesis provides the RM spectra for a single LOS pixel in a given data set. This means that by running the 1D RM-Synthesis on a single pixel for some given data, we will be able to determine the peak of the RM spectra for that pixel. Consider a single labelled pixel in the GALFACTS image from Fig. 3(a) as shown in Fig. 8. By performing a 1D RM-Synthesis on this pixel, the RM spectra can be generated as shown in Fig. 8. In this figure, the peak of the RM is given by the purple dashed line. We can use this peak RM value and compare it to Eq. 1 to determine the LOS magnetic field direction. As discussed in Sec. 3.2.2, the sign of the RM is decided by the magnetic field component of Eq. 1. In this case, the negative sign of the RM indicates that the LOS magnetic field component for this particular pixel is pointing away from the observer. It is also important to note that performing the 1D RM-Synthesis requires a range of frequency values as an input parameter. This is the reason that the radio observations from GALFACTS are employed for this part of the project.

4.2.2. 3D RM-Synthesis

Generalizing the process of the 1D RM-Synthesis, the peak of the RM can be determined for every pixel using the 3D RM-Synthesis. This is shown in Fig. 9 which displays the peak RM values for each pixel around G182.5-4.0. In this figure, areas of high RM values appear darker in their respective colour. The colours blue, white, and red are used to label the LOS magnetic field component that points away, in the POS, and towards the observer respectfully. Using this information, we can determine the direction of the LOS magnetic field as well as the POS magnetic field orientations from Eq. 1 and Eq. 2 respectfully. The POS field orientation will be given through the outputted de-roated angle data which can then be used as input parameters for a Line Integral Convolution (LIC) map. The purpose of a LIC map is to take angle data as a parameter which then outputs smooth and continuous vector orientations. Since one of the output files of the 3D RM-Synthesis contains de-rotated angle data (χ_0) for each pixel, it can be used as a parameter in order to generate a POS magnetic field LIC map. The result of this is shown in Fig. 11.

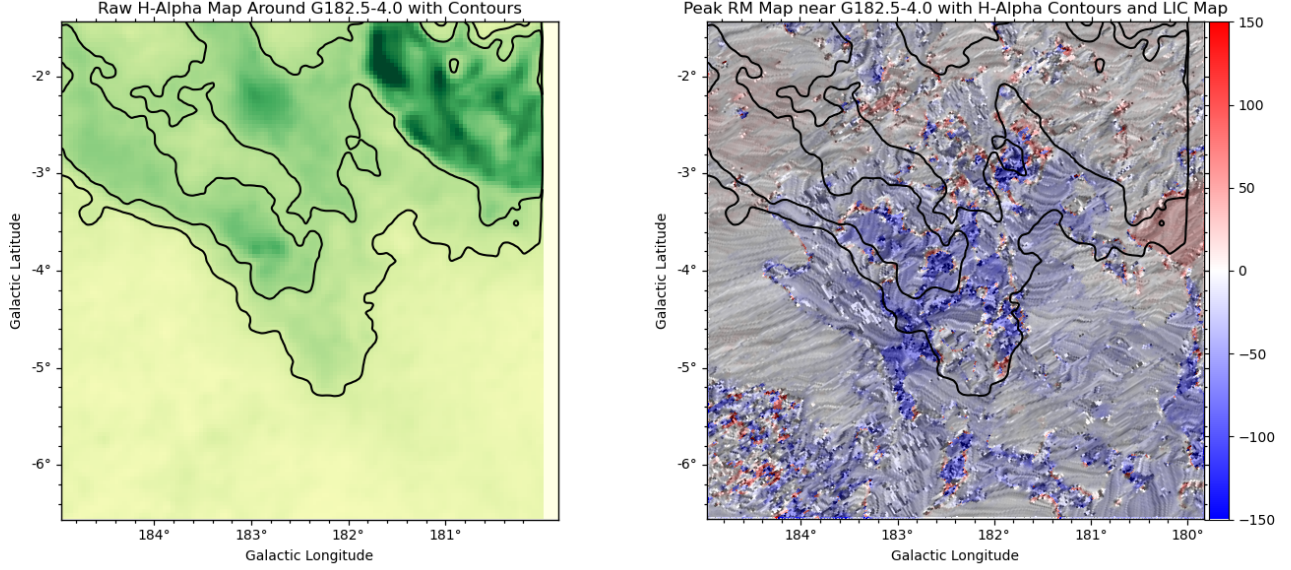


Figure 10. Regions of high intensities of $H\alpha$ represented as contours over-plotted on to the peak RM map (right). Also included is the LIC map in order to view the POS magnetic field orientation. It can be seen that the contour regions of $H\alpha$ contains a majority of the high negative peak RM values close to G182.5-4.0 as viewed from the LOS. This indicates a stronger contribution of thermal electron densities for RM values in this region. Also included is the raw $H\alpha$ map around G182.5-4.0 (left) for a visual aid.

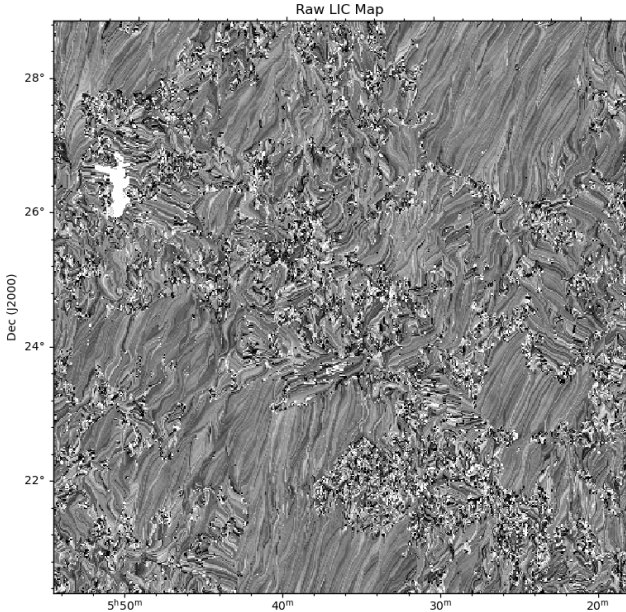


Figure 11. The raw LIC map which displays the POS magnetic field lines around G182.5-4.0. This map is generated by plotting a continuous vector field for which the orientation angles were given by an output file of the 3D RM-Synthesis.

5. DISCUSSION

5.1. Explaining Peak RM Values Near G182.5-4.0

Fig. 9(a) indicates high negative peak RM values near G182.5-4.0. From Fig. 11, a coherent POS magnetic field can be seen around the edges of the LIC map, while the center of the map displays incoherent linear vector structures. In order to explain the high value of $|RM|$ in the central region, consider the $H\alpha$ map in the region of G182.5-4.0 from Fig. 4.

The reason why this $H\alpha$ map is considered is because recalling from Eq. 1, RM values depend on the thermal electron density along with the LOS magnetic field component. If there are high intensities of $H\alpha$ in the region which we see greater RM values, this would indicate that the value of RM in a region is largely dominated by the thermal electron density component rather than the LOS magentic field component.

In Fig. 10, we overlay contours of greater intensities of this $H\alpha$ map onto the previous peak RM map from Fig 9(a), and also include the LIC map from Fig. 11. It can be seen that in the left-most and right-most areas where the high intensities of $H\alpha$ are not present, the RM values tend to be close to 0. Since there are low intensities of $H\alpha$ in these regions, this means that the RM values should be dominated by the LOS magnetic field component. However, even in the presence of low thermal electron densities, the RM values still tend to 0. This ultimately means that in these regions, there is both a low intensity of thermal electrons and less of

a LOS magentic field orientation. This indicates that the magnetic field in this region will be largely in the POS and that this POS magnetic field is the intrinsic magnetic field orientation, which is what is able to be observed by looking at the overlay of the LIC map in Fig. 10.

Areas where high intensities of $\text{H}\alpha$ are present can help to explain the abrupt shift in RM values, that tend to go from about 0 to high negative values going closer to G182.5-4.0. It can be seen from the $\text{H}\alpha$ contours in Fig. 10 that this change in RM values occurs past the boundary of the contours. This indicates that in the close vicinity of G182.5-4.0, the high negative values of RM found here are more likely due to higher intensities of $\text{H}\alpha$, and therefore thermal electrons in that region, and less likely due to a LOS magnetic field. This signifies that although there are large negative values for the RM in the close vicinity of G182.5-4.0, evidence from studying the $\text{H}\alpha$ intensities in this region indicates that there is most likely a minor component of a LOS magnetic field in this region, and that the remaining magentic field orientation is largely in the POS which is also the intrinsic orientation. This POS magnetic field appears to contain a coherent orientation. This is because ignoring the central region of Fig. 11, it can be seen that in the remaining part of this figure, a largely coherent and linear intrinsic POS magnetic field orientation can be seen in the non-central regions.

The conclusion is then that it is very likely that the orientation of the magnetic field in the entire region is similar to that of the magnetic field orientation in the non-central regions of Fig. 11. There may still be LOS components of the magentic field, but studying the $\text{H}\alpha$ intensities in this region suggests that the magnitude of these LOS components are significantly less than that of the POS components.

5.2. Comparing Orientation Angles

From Sec. 4.1, the average integrated orientation angle for the magnetic field along the POS was determined to be $101^\circ \pm 12^\circ$. Through performing RM-Synthesis, a LIC map containing the intrinsic POS magnetic field orientation was generated. In Fig. 12, we display both of these results simultaneously. In this figure, the filaments of G182.5-4.0 as seen through DRAO Stokes I have been included (green) as well as constant 101° lines (red). Comparing these orientations, it can be said that there is a strong correlation between both of these results. The matching orientations of the filaments of G182.5-4.0 and the 101° lines describe the results obtained from the RHT and polar plots. By over-plotting these results onto the LIC map, the 101° lines also co-

incide with the intrinsic POS magnetic field orientation from the LIC map.

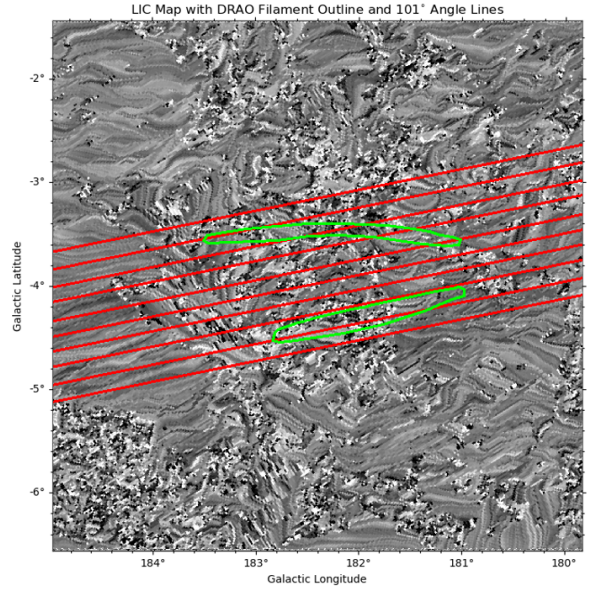


Figure 12. G182.5-4.0 DRAO Stokes I filaments (green) with 101° lines (red) over-plotted onto the LIC map which summarizes the final conclusion. The green and red orientations summarize the results of the RHT process while the LIC plot summarizes the process of RM-Synthesis. A strong connection between these three orientations can be seen which provides compelling evidence that the magentic field orientation is responsible for the structure of G182.5-4.0.

The result that this is highlighting is that the orientation of the filamentary structure of G182.5-4.0 strongly overlaps the intrinsic POS magnetic field orientation which is observed to permeate this object. This would then strongly imply that the structure of G182.5-4.0 has retained its shape due to the orientation of this interstellar magnetic field. From the results of this project, the hypothesis which is most favourable would be to classify G182.5-4.0 as filaments in the ISM that are a product of old SNR(s).

6. CONCLUSION

In conclusion, we have determined a strong correlation between the orientation of G182.5-4.0 and the magentic field in the surrounding region. Through employing the RHT, it was determined that the average orientation of HI filaments is $101^\circ \pm 12^\circ$. From performing the 3D RM-Synthesis, the peak RM values near G182.5-4.0 as well as χ_0 were determined. These peak RM values appear to be high negative values in the close vicinity of G182.5-4.0. Through studying the overlap of high intensities of $\text{H}\alpha$ in the same region, it was determined that these high negative peak RM values are more likely be-

ing produced by thermal electron densities rather than a LOS magnetic field component. This supports the idea of a coherent intrinsic POS magnetic field in which the orientation is given by a corresponding LIC map.

Through comparing the direction of the magnetic field from both the polarized (RM-Synthesis) and neutral (HI

filaments) mediums, and then mapping this with the structure of G182.5-4.0, a strong connection between these orientations is established at the orientation angle of $101^\circ \pm 12^\circ$. From these results, the current hypothesis for the structure of G182.5-4.0 is that this object has achieved its shape due to the galactic magnetic field which is known to permeate the surrounding region

REFERENCES

- Brentjens, M.A., de Bruyn, A.G., 2005, A&A, 441, 1217
- Clark, S. E., Peek, J. E. G., Putman, M. E., 2014, APJ, 1-2, 4
- Ferriere, K., 2012, EAS, 24
- Finkbeiner, D. P., 2003, ApJS, 146, 407.
- Han, J.L., 2017, ARAA, 112, 136-138
- Heald, G., 2008, IAU
- Igumenshchev, I. V., Tutukov, A. V., Shustov, B. M., 1992, SOVAST, 245
- Landecker, T. L., Dewdney, P. E., Burgess, T. A., et al. 2000, A&AS, 145, 509.
- Lopez, L. A., arXiv:1306.2638, 2-3
- Newton-McGee, K. J., 2009, School of Physics University of Sydney, 6-7, 21
- Taylor, R., Salter, Chris., 2010, arXiv:1008.4944v1
- Wallace, B.J., Landecker, T. L., Kalberla, P. M. W., Taylor, A. R., APJS, 3
- West, J., Kothes, R., Safi-Harb, S., 2020, University of Toronto, Dunlap Institute for Astronomy & Astrophysics
- Xiao, L., Furst, E., Reich, W., Han, L. J., 2008, A&A, 1